2016 24th Iranian Conference on Electrical Engineering (ICEE)

Experimental Evaluation of a Saturated Output Feedback Controller Using RBF Neural Networks for SCARA Robot IBM 7547

Mohammad Pourrahim Khoshnam Shojaei Abbas Chatraei Omid Shah Nazari

Department of Electrical Engineering
Najafabad Branch, Islamic Azad University
Najafabad, Iran

Email: {pde.mohammad, khoshnam.shojaee, abbas.chatraei, dep.omid@gmail.com}

Abstract—**In this paper, an extension of the passivity-based output feedback trajectory tracking controller is addressed and implemented on a SCARA robot IBM 7547 by using generalized saturation. Compared with the output feedback controllers, a radial basis function saturated observer-based controller has been introduced. The controller will reduce the risk of actuator saturation effectively via generalized saturation functions. Implementation results are provided to illustrate the efficiency of the proposed controller in dealing with the actuator saturation.**

Keywords-Output feedback controller; RBF Neural Networks; SCARA robot; Generalized saturation; robot manipulator.

I. INTRODUCTION

The design of nonlinear controllers suitable for real-time control of multiple-input–multiple-output (MIMO) nonlinear systems is one of the most challenging tasks for many control researches. A robot manipulator is an uncertain nonlinear dynamic MIMO system which suffers from structured and unstructured uncertainties such as payload variation, friction, external disturbances, etc. In the last few decades, artificial intelligent control using fuzzy logic systems (FLS) and neural networks (NN) has undergone a rapid development to design feedback controllers for complex systems. A lot of works have been carried out in the field of control of robot manipulators using NN-based controllers which require both position and velocity measurements ([1-3]). In [4], a neuro adaptive hybrid controller has been proposed for robot manipulator tracking control in which three multilayer neural networks are used to learn the inertia matrix, Coriolis vector and the gravitational torque vector, respectively. It, however, suffers from computational complexity. In other research, sliding mode-based control system has been realized to solve trajectory tracking problem of robot manipulator in which two NNs are used to approximate equivalent and switching control terms, respectively [5]. In the same direction, Wai in [3] presented a sliding mode neural network control system for position control of robotic manipulators in which a NN controller is developed to estimate the equivalent control part. The robot control problem has also been addressed using combined and uncombined methods. In [6], a simple adaptive control has been proposed for the robot tracking problem satisfying actuator constraints without using velocity measurement such that for estimating the structured/ unstructured uncertainties a CNN has been presented. In this work, local asymptotic convergence whit a rather large region of feedback controller has been proposed for a class of large-scale time-delay systems input constraints. This controller is based on the backstepping method combining with DSC technology, RBF neural networks and the auxiliary system. This research proves that tracking errors of the system converge to a small neighborhood.

From a practical viewpoint, the actuator saturation problem should be taken into account in designing control systems. If the actuator is saturated, the control system may show a poor tracking performance. Furthermore, long-term saturation may lead to serious physical damage or to thermal or mechanical failure of the system actuators. One solution to alleviate this problem is bounding of the closed-loop error variables by applying saturation functions in designing the tracking controller. For example, saturation and hyperbolic tangent functions have been utilized to design bounded tracking control laws for robotic manipulators [8-9] in which a RBFNN has been employed in controller scheme. In this paper, the experimental evaluation of a saturated output feedback control scheme using RBF neural network for SCARA robot IBM 7547 is presented.

The remainder of this paper is organized as follows. In Section II, some preliminaries are presented briefly. A saturated output feedback tracking control system is presented in Section III. The experimental results are provided in Section IV to evaluate the effectiveness of the proposed controller. Eventually, Section V contains the Conclusion.

II. PROBLEM FORMULATION

A. Robot dynamics

Using the Euler–Lagrangian formulation, the dynamics of robot manipulators with rigid links can be written as:

$$M(q)\ddot{q} + C(q,\dot{q})\dot{q} + D(q)\dot{q} + G(q) = \tau_a \tag{1}$$

where $q \in R^n$ is the joint variable vector, whose entries are

This research has been supported by robotics center of Islamic Azad University, najafabad branch. (IAUN)

robot arm joint angles or link extensions. $M(q) \in R^{n\times n}$ is a symmetric positive-definite inertia matrix, $C(q,\dot{q}) \in R^{n\times n}$ is the centripetal and Coriolis matrix, and $D(q)$ is a strictly positive definite matrix. The vector $G(q) \in R^{n}$ represents gravity effects and the control input torque is $\tau_a \in R^n$.

Property 1. M(q) is a symmetric and positive-definite matrix that is upper and lower bounded such that $\lambda_M \|x\|^2 \le x^T M(q) x \le \lambda_M \|x\|^2 \ \forall x, q \in R^n$ and $0 < \lambda_m \le \lambda_M < \infty$, where $\lambda_M := \min_{\forall q \in R^n} \lambda_{min}\left(M(q)\right) and\ \lambda_M := \max_{\forall q \in R^n} \lambda_{max}\left(M(q)\right)$ [10].

Property 2. The Coriolis matrix satisfies following properties [10]:

2.1) $x^T\left(\dot{M}(q,\dot{q}) - 2C(q,\dot{q})\right)x = 0,\ \forall x, q, \dot{q} \in R^n;$

2.2) $\dot{M}(q,\dot{q}) = C(q,\dot{q}) + C^T(q,\dot{q}),\ \forall q, \dot{q} \in R^n;$

2.3) $C(q,x_1)x_2 = C(q,x_2)x_1,\ \forall x_1, x_2, q \in R^n;$

2.4) $C(q, x_1 + x_2)y = C(q,x_1)y + C(q,x_2)y,$ $\forall q, x_1, x_2, y \in R^n;$

2.5) $\|C(q,x_1)x_2\| \le \lambda_C \|x_1\| \|x_2\|,\ \forall x_1, x_2, q \in R^n$ for some constant $\lambda_C \ge 0$.

Property 3. The gravity vector can be upper bounded as $\|G(q)\| \le \lambda_G,\ \forall q, \dot{q} \in R^n$, where λ_G is a positive scalar constant that is known or may be approximated by an expert designer.

Property 4. The matrix *D(q)* is a symmetric and positive-definite matrix that satisfies $\lambda_d \|x_2\|^2 \le x^T D(q) x \le \lambda_d \|x_2\|^2 \ \forall\, x \in R^n$ and $0 < \lambda_d \le \lambda_D < \infty$, where $\lambda_d := \min_{\forall q \in R^n} \lambda_{min}\left(D(q)\right) and\ \lambda_D := \max_{\forall q \in R^n} \lambda_{max}\left(D(q)\right)$.

Property5 [11]. There exist positive constants $\zeta_M, \zeta_c, \zeta_D$ and ζ_G for all $q, q_d, \dot{q_d} \in R^n$ such that

$$\begin{aligned} &\|M(q) - M(q_d)\| \le \zeta_M \|s(q - q_d)\| \\ &\|C(q,\dot{q_d}) - C(q_d,\dot{q_d})\| \le \zeta_C \|\dot{q_d}\| \|s(q - q_d)\| \\ &\|D(q) - D(q_d)\| \le \zeta_D \|s(q - q_d)\| \\ &\|G(q) - G(q_d)\| \le \zeta_M \|s(q - q_d)\| \end{aligned} \tag{2}$$

Assumption 1. Measurements of output vector $q \in R^n$ are available in real-time.

Assumption 2. The desired trajectory $q_d(t)$ is chosen such that $q_d(t)$, $\dot{q_d}(t)$, and $\ddot{q}_d(t)$ are all bounded signals in the sense that $\sup_{t\ge0}\|q_d\| < B_{dp}$, $\sup_{t\ge0}\|\dot{q_d}\| < B_{dv}$, and $\sup_{t\ge0}\|\dot{q_d}\| < B_{da}$, where B_{dp}, B_{dv}, and B_{da} are bounded constants.

Definition 1. Given a positive constant M_i, a function $s_i: R \to R: \xi \to s_i(\xi)$ is said to be a generalized saturation one with bound M_i, if it is locally Lipschitz, non-decreasing, and satisfies (i) $\xi s_i(\xi) > 0, \forall \neq 0$; (ii) $|s_i(\xi)| \le M_i, \forall \xi \in R$.
The following generalized saturation function is considered as a candidate in this paper:

$$s_j(\eta_j) = \begin{cases} -L_j + (M_j - L_j)\tanh\left(\frac{\eta_j + L_j}{M_j - L_j}\right), \forall \eta_j < -L_j \\ \eta_j, \qquad\qquad\qquad\qquad\qquad \forall \eta_j < -L_j \\ L_j + (M_j - L_j)\tanh\left(\frac{\eta_j - L_j}{M_j - L_j}\right), \forall \eta_j < -L_j \end{cases} \tag{3}$$

where M_j and L_j are constants such that $L_j < M_j$.
The proof of properties is easily accomplished by following in references [12, 13].

B. RBFNN approximator

In this subsection, RBFNN is introduced as an approximator of uncertain nonlinearities of robot dynamics. Fig. 1 shows the structure of a three-layer RBFNN. This structure is widely used to estimate unknown functions [14].

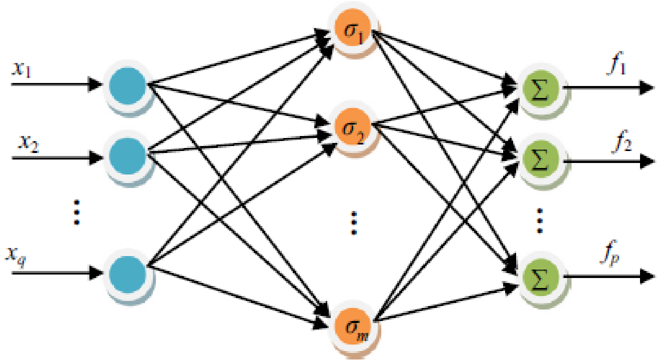

Fig. 1. The structure of radial basis function neural network.

In RBFNN, the activation function is given as follows:

$$\begin{aligned} f_m(x) &= \sum_{k=1}^{\ell} W_{mk}\,\sigma_k(x) \qquad m = 1,2, \dots, p, \\ \sigma_k(x) &= \exp\left(-\frac{\|x - \mu_k\|^2}{\lambda_k^2}\right) \qquad k = 1,2, \dots, \ell \end{aligned} \tag{4}$$

where ℓ and p are the number of hidden and output nodes, respectively, $\sigma_k(x)$ is k-th Gaussian basis function where $\mu_k = [\mu_{k2}, \mu_{k1}, \dots, \mu_{kq}]^T$ and λ_k are the center vector and the standard deviation, respectively. Then, the approximated nonlinearities can be expressed as follows:

$$f(x) = W\sigma(x) \tag{5}$$

where $f(x) = [f_1(x), \dots, f_p(x)]^T$, $W \in R^{p\times\ell}$ is the weight and $\sigma(x) = [\sigma_1(x), \dots, \sigma_\ell(x)]^T$. Let us define $\hat{f}$ as the estimate of the uncertain nonlinearities, given by $\hat{f}(x) = \widehat{W}\sigma(x)$, where $\widehat{W}$ denotes the estimated weight matrix which is updated by an appropriate update rule.

III. CONTROLLER DESIGN

In this subsection, a saturated output feedback controller is designed based for the model given in[12]. For the observer design purposes, the tracking error is defined as $e(t) = q(t) - q_d(t)$ and the observation error is denoted by $z(t) = q(t) - \hat{q}(t)$, where $\hat{q}(t)$ is the estimate of $q(t)$. Then, consider the following definitions:

$$\dot{q}_r = \dot{q}_d - \Lambda s(q - q_d) = \dot{q}_d - \Lambda s(e) \tag{6}$$

$$r_1 = \dot{q} - \dot{q}_r = \dot{e} + \Lambda s(e) \tag{7}$$

$$\dot{q}_o = \dot{\hat{q}} - \Lambda s(z) \tag{8}$$

$$r_2 = \dot{q} - \dot{q}_o = \dot{z} + \Lambda s(z) \tag{9}$$

where $q_r(t),\ q_o(t) \in R^{n\times n}$ are the controller and observer variables, respectively, and $\Lambda \in R^{n\times n}$ is a symmetric positive definite gain matrix. By substituting (7) into (1), one obtains

$$M(q)\dot{r}_1 = -C(q,\dot{q})r_1 - D(q)r_1 + \tau_a - C(q,\dot{q}_r)\dot{e} + C(q,\dot{q}_d)\Lambda s(e) + M(q)\Lambda s'(e)\dot{e} + D(q)\Lambda s(e) + \tilde{\xi} - \xi_d \tag{10}$$

where

$$\tilde{\xi} = \big(M(q_d) - M(q)\big)\ddot{q}_d + \big(C(q_d,\dot{q}_d) - C(q,\dot{q}_d)\big)\dot{q}_d + \big(D(q_d) - D(q)\big)\dot{q}_d + G(q_d) - G(q)$$

which can be bounded as $\|\tilde{\xi}\| \le B_\xi \|s(e)\|$ via Property 5, where $B_\xi = \zeta_M B_{da} + \zeta_c B_{dv}^2 + \zeta_G$. In addition, $\xi_d = M(q)\ddot{q} + C(q,\dot{q})\dot{q} + D(q)\dot{q} + G(q)$ denotes the desired computed system dynamics, which is written as $\xi_d = W\sigma(x)$. Then, the following saturated output feedback controller is proposed in this paper:

$$\tau_a(t) = -s(K_1\dot{q}_o - K_1\dot{q}_r) + \widehat{W}\sigma(x) \tag{11}$$

where $K_1 \in R^{n\times n}$ is a symmetric positive-definite gain matrix and NN weights are updated by the following adaptation rules which will be derived in the next subsection:

$$\dot{\widehat{W}} = F\sigma e_p - KF\|e_p\|\widehat{W} \tag{12}$$

where $F = F^T > 0$ and $K > o$ is small constant design parameter. In order to make the adaptive rule independent from velocity measurements, the term e_p is substituted with $e_p = \dot{\hat{q}} - \dot{q}_d + \Lambda s(e) + \Lambda s(z)$.

Remark1. In fact, this approximation $r_1 + r_2 \cong \hat{r}_1 + \hat{r}_2 = e_p$ can be verified if the controller observer gains k_d, Λ are set large enough so k_d is the observer gain, which is defined later. The interested reader is referred to [9] for a similar discussion on this approximation. As a result, the following adaptive rule is introduced:

$$\dot{\widehat{W}} = F\sigma(\dot{\hat{q}} - \dot{q}_d + \Lambda s(e) + \Lambda s(z))^T - KF\|\dot{\hat{q}} - \dot{q}_d + \Lambda s(e) + \Lambda s(z)\|\widehat{W} \tag{13}$$

Then, considering that $r_1 - r_2 := \dot{q}_o - \dot{q}_r$ from (8) and (10) and substituting (12) into (13), the closed-loop system error dynamic is achieved as follows:

$$M(q)\dot{r}_1 = -C(q,\dot{q})r_1 - D(q)r_1 - s(K_1r_1 - K_1r_2) + \widetilde{W}\sigma(x) + X_1 \tag{14}$$

where $\widetilde{W} = \widehat{W} - W$ and

$$X_1 = -C(q,\dot{q}_r)\dot{e} + C(q,\dot{q}_d)\Lambda s(e) + M(q)\Lambda s'(e)\dot{e} + D(q)\Lambda s(e) + \tilde{\xi} \tag{15}$$

One may obtain the following upper bound for $X_1 \in R^n$:

$$\|X_1\| \le \xi_1\|X\| + \xi_2\|X\|^2 \tag{16}$$

where $\xi_1, \xi_2 \in R$ are some positive bounding constants and $X \in R^{4n}$ is defined as:

$$X := [S^T(e), S^T(z), r_1^{\mathrm{T}}, r_1^{\mathrm{T}}] \tag{17}$$

Motivated by [1], the following velocity observer is proposed in this paper:

$$\dot{\hat{q}}(t) = \dot{\hat{q}}_o(t) + \Lambda s(z(t)) + k_d z(t) \tag{18}$$

$$\dot{\hat{q}}_o(t) = \dot{q}_d(t) + k_d\Lambda\int_0^t s(z(\tau))\,d\tau \tag{19}$$

where $k_d \in R$ is the observer gain, which is a positive real constant. The initial conditions for the observer are chosen as $\dot{\hat{q}}_o(0) = -\Big(\Lambda s\big(z(0)\big) + k_d z(0)\Big)$ and $\hat{q}(0) = q(0)$ to have $z(0) = 0$ and $\dot{\hat{q}}(0) = 0$. Differentiating (19) results in $\ddot{\hat{q}} = \ddot{\hat{q}}_o + \Lambda\acute{S}(e)\dot{e} + k_d\dot{z}$, which is equivalent to $\dot{r}_1 = \dot{r}_1 + k_d r_2 + \Lambda\acute{S}(e)\dot{e}$ by substituting (7), (9), and (19). This equation, together with (14) and properties in the previous section, yield the following observer error equation:

$$M(q)\dot{r}_2 = -C(q,\dot{q})r_1 - D(q)r_1 - s(K_1r_1 - K_1r_2) + \widetilde{W}\sigma(x) + X_2 \tag{20}$$

where

$$X_2 = -D(q)r_1 + D(q)\Lambda s(e) + C(q, r_1 + \dot{q}_r)r_2 - C(q,r_1)(r_1 + 2\dot{q}_r) + C\big(q,\Lambda s(e)\big)(\dot{q}_r + \dot{q}_d) + \tilde{\xi} \tag{21}$$

the following upper bound for $X_2(e,z,r_1,r_2)$ is obtained:

$$\|X_2\| \le \xi_3\|X\| + \xi_4\|X\|^2 \quad (22)$$

where $\xi_3, \xi_4 \in R$ are some positive bounding constants.
The stability proof is easily accomplished by following the stability proofs in references [12] and [14].

IV. EXPERIMENTAL EVALUATION

In this section, the proposed neural network controller is implemented on a SCARA robot available in robotic center of IAUN. As show in figure 4, this SCARA IBM 7547 is a 4 DOFs RRPR robot. The workspace of this robot has been illustrated in figure 6.

A. SCARA KINEMATICS

Through Denavit-Hartenberg convention and according to assigned frames which show in figure 2, the equation of forward kinematic of SCARA robot is derived as follows:

$$\begin{bmatrix} R & P \\ 0 & 1 \end{bmatrix} = \begin{bmatrix} C_{12}C_4 + S_{12}S_4 & SC_4 - C_{12}S_4 & 0 & a_1C_1 + a_2C_{12} \\ S_{12}C_4 - C_{12}S_4 & -C_{12}C_4 - S_{12}S_4 & 0 & a_1S_1 + a_2C_{12} \\ 0 & 0 & -1 & -d_3 - d_4 \\ 0 & 0 & 0 & 1 \end{bmatrix} \quad (23)$$

where R and P represent the orientation and position of last frame w.r.t first frame, respectively. Hence, the following equations will be used as forward kinematics of the robot:

$$P_x = a_1C_1 + a_2C_{12}$$

$$P_y = a_1S_1 + a_2C_{12}$$

$$P_z = -d_3 - d_4$$

In order to obtain the equation of inverse kinematics of SCARA robot, one can the following equation according to figure 2 and some geometric rules [15].

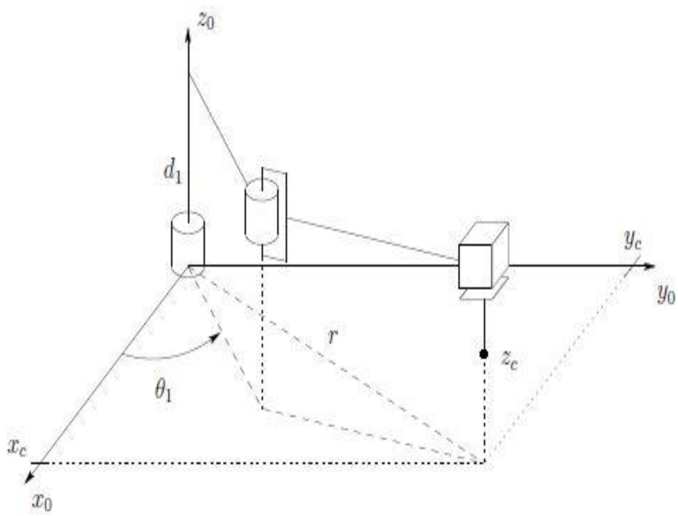

Fig. 2. Configuration of SCARA robot on $x_0 - y_0$ plane.

$$\theta_2 = Atan(c_2, \pm\sqrt{1 - c_2}) \quad (24)$$

$$c_2 = \frac{O_x^2 + O_y^2 - a_1^2 - a_2^2}{2a_1a_2} \quad (25)$$

$$\theta_1 = Atan(O_x, O_y) - Atan(a_1 + a_2c_2, a_2s_2) \quad (26)$$

$$\theta_4 = \theta_1 + \theta_2 - \alpha = \theta_1 + \theta_2 - Atan(r_{11}, r_{12}) \quad (27)$$

$$d_3 = O_z + d_4 \quad (28)$$

B. EXPERIMENTAL RESULTS

In this subsection, the proposed controller is experimentally evaluated on a real manipulator system. SCARA IBM 7547 robot has 4 DC motor equipped with 4 encoders whose first and second motors have gearbox. These motors are derived with a 600W, 4 channel driving board, while the control system the robot has been designed and implemented on an Arduino Due board which is based on Atmel SAM3X8E ARM cortex-M3 CPU (as show in figure 5).
The following control parameters are applied to the proposed controller in order to evaluate its performance:
$M_j = 4, L_j = 0.9, k_d = 10, \Lambda = 20, K_1 = 1.1.$

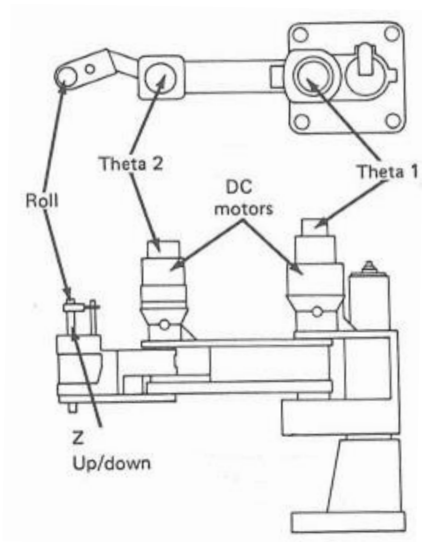

Fig. 3. IBM 7540 SCARA Components.

Fig. 4. SCARA IBM 7547 robot manipulator.

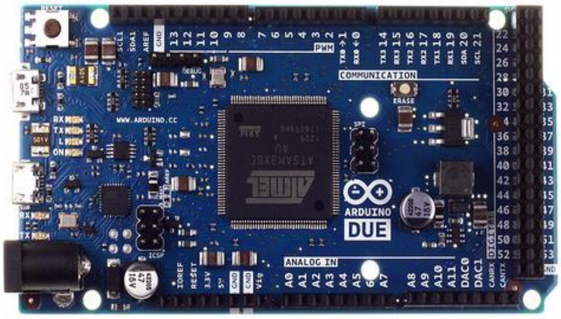

Fig. 5. Controller hardware base on Arduino Due.

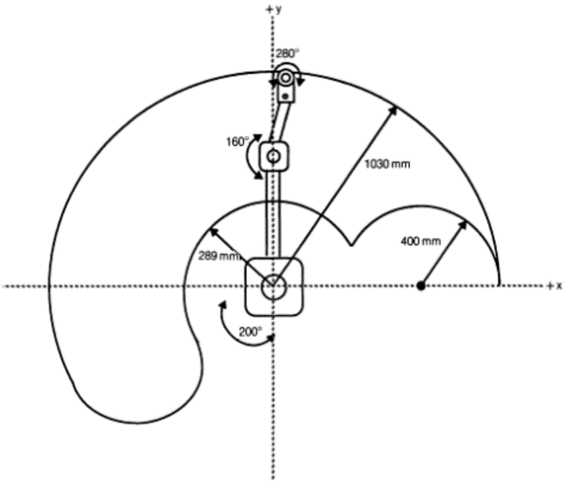

Fig. 6. Workspace of SCARA robot IBM 7547.

The tracking performance of the control system is illustrated in figure 7. The desired task trajectory is a circle whose origin and radius are given by (0,0.63) m and 0.2 m, respectively, in horizontal plane.

In this research, the proposed controller is implemented only on the first and second joints of the manipulator for the simplicity. Figure 8 and 9 show the control inputs of first and second joints of the robot respectively.

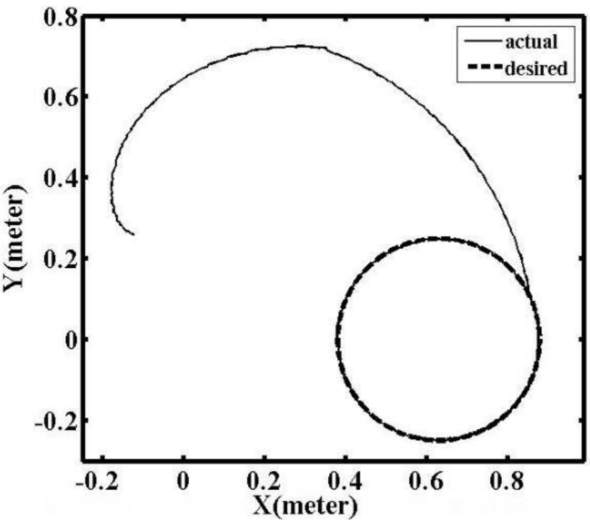

Fig. 7. X-Y plot of the desired trajectory and SCARA trajectory with generalized saturation.

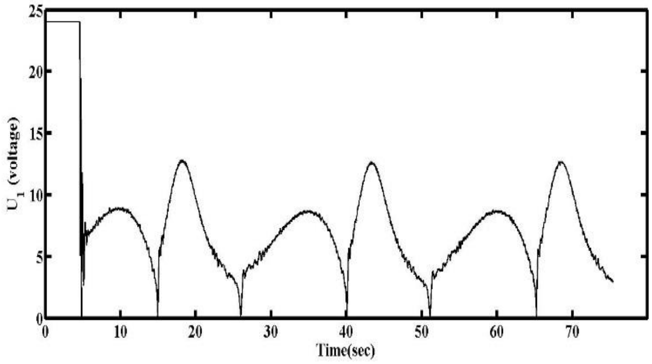

Fig. 8. Signal control Joints 1 with generalized saturation.

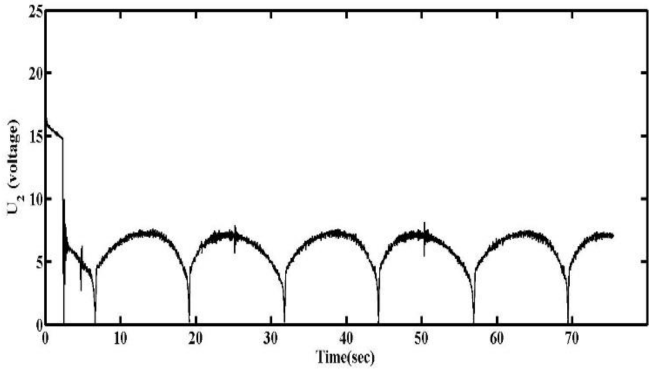

Fig. 9. Signal control Joints 2 with generalized saturation.

The output tracking error of first and second joint are shown in figures 10, 11 respectively.

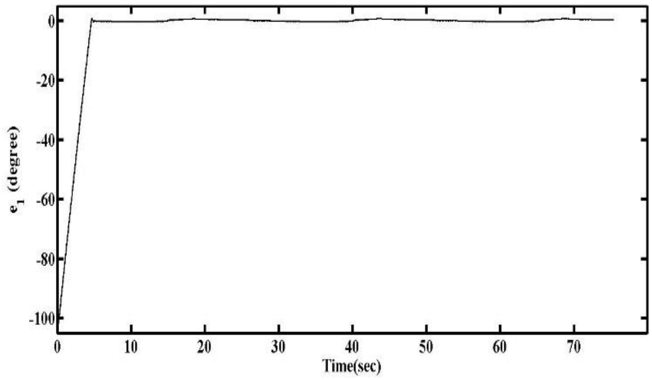

Fig. 10. Output tracking error Joints 1 with generalized saturation.

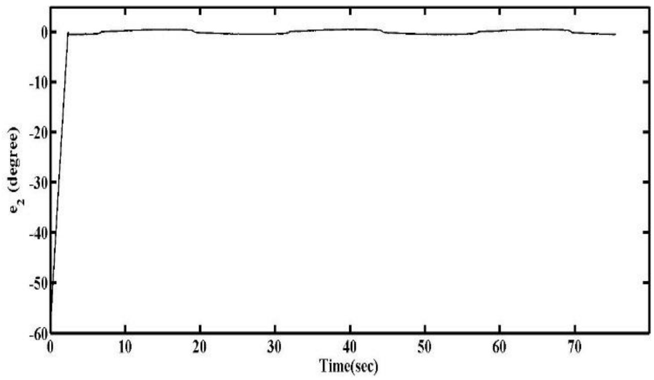

Fig. 11. Output tracking error Joints 2 with generalized saturation.

The estimated errors of first and second joints are depicted in figures 12 and 13, respectively.

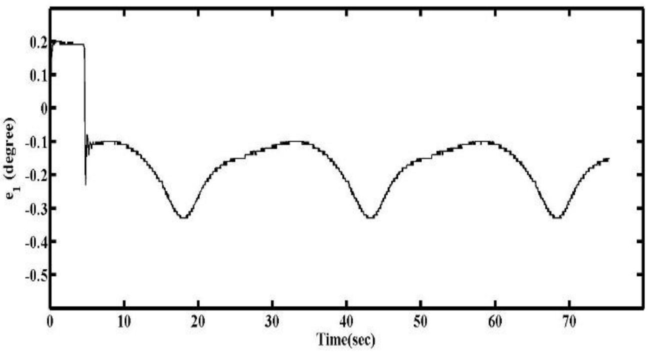

Fig. 12. Estimate error Joints 1 with generalized saturation.

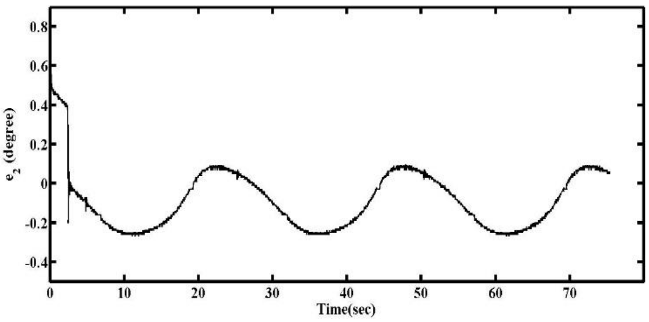

Fig. 13. Estimate error Joints 2 with generalized saturation.

Eventually, the rate of estimated errors of both joints are shown in figures 14 and 15.

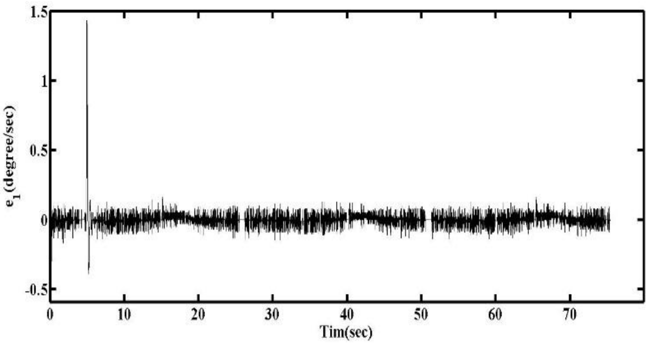

Fig. 14. Angular velocity estimation error Joints 1 with generalized saturation.

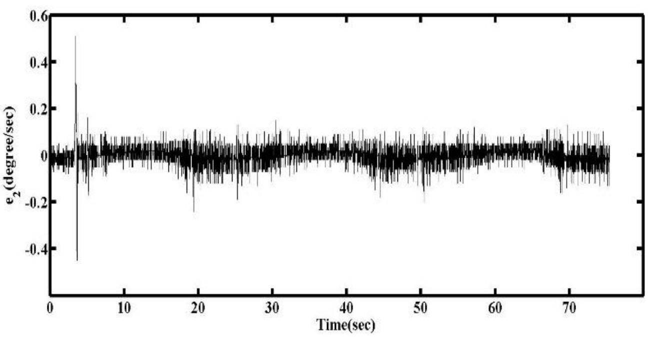

Fig. 15. Angular velocity estimation error Joints 2 with generalized saturation.

V. CONCLUSION

In this paper, the output feedback tracking control problem of the robot SCARA IBM 7547 in the presence of actuator constraints has been addressed. Generalized saturation functions have been utilized effectively to implement a novel passivity-based output feedback tracking controller. This, in turn, improves the transient performance for large initial tracking errors in the trajectory tracking problem. Moreover, the proposed controller can compensate for parametric uncertainties without velocity measurements.

For the purpose of experimental implementation, the proposed output feedback tracking controller is applied to a 4-DOFs SCARA robot manipulator. Experimental results successfully showed that the proposed controller effectively copes with the tracking problem in the presence of actuators constraints and model uncertainties.

REFERENCES

[1] Barambones, Oscar, and Victor Etxebarria. "Robust neural control for robotic manipulators." Automatica, Vol. 38, No. 2, pp. 235-242 (2002).

[2] Lewis, Frank L., Aydin Yesildirek, and Kai Liu. "Multilayer neural-net robot controller with guaranteed tracking performance." Neural Networks, IEEE Transactions on,Vol. 7, No. 2, pp. 388-399 (1996).

[3] Wai, Rong-Jong. "Tracking control based on neural network strategy for robot manipulator." Neurocomputing, Vol. 51, No. 3, pp. 425-445 (2003).

[4] s Behera, L., S. Chaudhury, and M. Gopal. "Neuro-adaptive hybrid controller for robot-manipulator tracking control." IEE Proceedings-Control Theory and Applications, Vol. 143, No. 2, pp. 270-275 (1996).

[5] Ertugrul, Meliksah, and Okyay Kaynak. "Neuro sliding mode control of robotic manipulators." Mechatronics, Vol. 10, No. 1, pp. 239-263 (2000).

[6] Purwar, Shubhi, Indra Narayan Kar, and Amar Nath Jha. "Adaptive output feedback tracking control of robot manipulators using position measurements only." Expert systems with applications, Vol. 34, No. 4, pp. 2789-2798 (2008).

[7] Le, Tien Dung, and Hee-Jun Kang. "An adaptive tracking controller for parallel robotic manipulators based on fully tuned radial basic function networks." Neurocomputing, Vol. 137, No.5, pp. 12-23 (2014).

[8] Santibanez, V., K. Camarillo, J. Moreno-Valenzuela, and R. Campa "A practical PID regulator with bounded torques for robot manipulators." Int. J. Control Autom.Syst., Vol. 8, No. 3, pp. 544–555 (2010).

[9] Su, Y., P. Muller, and C. Zheng "Global asymptotic saturated PID control for robotmanipulators," IEEE Trans.Control Syst. Technol., Vol. 18, No. 6, pp. 1280–1288 (2010).

[10] Arteaga, Marco, and Rafael Kelly. "Robot control without velocity measurements: New theory and experimental results." Robotics and Automation, IEEE Transactions on, Vol. 20, No. 2, pp. 297-308 (2004).

[11] Huang, C. Q., X. F. Peng, C. Z. Jia, and J. D. Huang "Guaranteed robustness/performance adaptive control with limited torque for robot manipulators, " Mechatronics, Vol. 18, pp. 641–652 (2008).

[12] Khoshnam Shojaei, and Abbas Chatraei. "A Saturating Extension of an Output Feedback Controller for Internally Damped Euler-Lagrange Systems." Asian Journal of Control, Vol. 18, No. 2, pp. 1–13 (2016).

[13] Aguinaga-Ruiz, E., A. Zavala-Rio, V. Santibanez, and F. Reyes "Global trajectory tracking through static feedback for robot manipulators with bounded inputs," IEEE Trans. Control Syst. Technol., Vol. 17, No. 4, pp. 934–944 (2009).

[14] Lewis, Frank L., Darren M. Dawson, and Chaouki T. Abdallah. Robot manipulator control: theory and practice. CRC Press, (2003).

[15] Spong, Mark W., and Mathukumalli Vidyasagar. Robot dynamics and control. John Wiley & Sons, (2008).